

## Observation of high-frequency secondary modes during strong tearing mode activity in FTU plasmas without fast ions

P. Buratti, P. Smeulders, F. Zonca, S.V. Annibaldi, M. De Benedetti, H. Kroegler, G. Regnoli, O. Tudisco and the FTU-team,

EURATOM-ENEA Association, C.R. Frascati, CP 65, 00044 Frascati, Italy.

e-mail contact of main author: buratti@frascati.enea.it

**Abstract.** MHD spectroscopy in FTU has revealed high frequency (HF) oscillations between 30 and 70 kHz that accompany the development of large  $m=-2$ ,  $n=-1$  islands in ohmic plasmas. This frequency range is one order of magnitude above the island rotation frequency, one order of magnitude below the first toroidal gap in the Alfvén continuum and of the same order of the low frequency gap introduced by finite beta effects. The HF spectrum is organized in pairs of modes with opposite toroidal numbers,  $n=1$  and  $n=-1$  for the stronger ones, which form standing waves in the island rest frame. The poloidal structure of HF modes appears to vary from  $|m|=2$  on the low field side to  $|m| \sim 5-6$  on the high field side. HF lines appear when the level of poloidal field perturbation produced by the island at the plasma edge exceeds 0.2%. The absence of energetic ions in FTU ohmic plasmas, the strict correlation between HF and tearing modes and the existence of a threshold indicate that HF modes tap energy either from the tearing mode by a non-linear mechanism or from fast electrons.

### 1. Introduction

High frequency oscillations in magnetically confined plasmas have been identified as discrete Alfvén eigenmodes (AE) excited by high-energy ions [1]. Frequencies of discrete AE stay in gaps that are introduced in the shear Alfvén continuum by poloidal mode coupling due to toroidicity, ellipticity and other equilibrium features. AE typically have much larger frequencies than other plasma instabilities such as tearing modes or fishbones. The frequency of toroidicity induced Alfvén eigenmodes (TAE) is  $\omega_{TAE} = \omega_A / 2 = V_A / (2qR)$ , where  $V_A$  is the Alfvén velocity,  $q$  the safety factor and  $R$  the major radius. Other gaps introduced by equilibrium features have even higher frequencies. Energetic ion losses due to Alfvén waves at frequencies below  $\omega_{TAE}$  have been found in some experiments [2]. These waves have been named BAE (beta-induced Alfvén eigenmodes) since their frequency is located in a gap  $0 < (\omega / \omega_A)^2 < \gamma \beta q^2$  [1], which is caused by finite plasma compressibility. Here  $\gamma$  is the ratio of specific heats and  $\beta$  the ratio of kinetic and magnetic pressures. While experimental evidence of BAE modes was originally due to the circulating fast ion population [2], the main effect of such fluctuations in a burning plasma will be from trapped alpha particles, due to their low frequency. [3, 4] The low frequency shear Alfvén gap also appears to be the explanation of the low frequency feature of Alfvén Cascades in JET [5].

MHD spectroscopy measurements in FTU have revealed the existence of high frequency (HF) waves in ohmic plasmas. HF waves appear as a multiplicity of lines between 30 kHz and 70 kHz (FIG. 1), whereas the oscillation frequencies associated with tearing modes is typically below 5 kHz, with weaker harmonics extending up to 20 kHz. The frequency range of HF waves is one order of magnitude below  $\omega_{TAE}$  and of the same order of the gap introduced by finite beta effects. The latter is sometimes indicated as the low frequency gap; we avoid this term since in this context low frequency means tearing mode frequency, i.e. below 20 kHz. There is a clear causal relationship between the development of large magnetic islands produced by  $m=2$ ,  $n=1$  tearing modes and the appearance of HF waves in FTU, in fact the latter only appear above a threshold island amplitude, as discussed in Section 2. The observation of HF waves in ohmic plasmas, where high-energy ions are absent, calls for the

identification of a new energy source from which HF waves tap energy. Possible explanations of HF modes excitation in the presence of magnetic islands are outlined in Section 3.

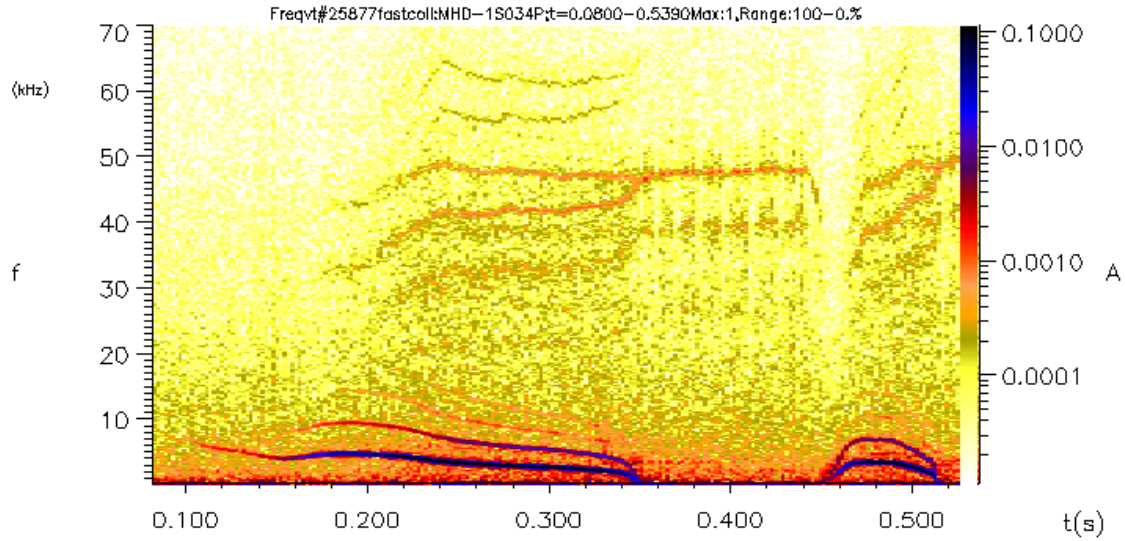


FIG. 1. Spectrogram of a Mirnov coil at  $34^\circ$  above the midplane in FTU ohmic pulse 25877 with  $B=5.9T$ ,  $I_p=0.49MA$ ,  $n=0.4$ . The current flat top starts at  $t=0.15$  s. Ordinates and colorscale indicate frequency in kHz and amplitude  $\delta B_{pol} / B_{pol}$  respectively. Intense lines below 20 kHz correspond to a  $(-2,-1)$  tearing mode and its “temporal” harmonics. The HF line near 50 kHz has  $n=-1$ ; the other just below has  $n=1$ .

## 2. Experimental results

FTU is a compact, high field tokamak, with major radius  $R=0.935$  m, minor radius  $a=0.3$  m and maximum magnetic field  $B=8$  T. Magnetic activities are analysed by means of a set of magnetic coils. A total of 57 poloidal field pick-up coils are installed at various toroidal and poloidal positions. Only 16 channels are at present recorded by the fast data acquisition system over 1.8 sec at 500 kHz with anti-aliasing. The minimum separation in poloidal angle is  $5^\circ$ , so that the maximum poloidal mode number that can be dealt with is 72. Similarly the toroidal separation is  $15^\circ$  allowing for a maximum toroidal mode number of 24. Internal measurements on island structure and amplitude are available from soft x-ray and electron cyclotron emission (ECE) diagnostics.

HF modes were first observed in discharges with low density and edge safety factor  $q_a > 5$ . In these discharges magnetic islands formed by tearing instabilities around the  $q=2$  surface can saturate at large amplitudes without provoking disruptions [6], so that the development of HF modes can be studied at nearly steady-state conditions. HF modes have been recently observed in other (transient) conditions, for example during disruption precursors.

### 2.1. MHD spectra

The typical frequency of magnetic oscillations produced by island rotation (island frequency in short) is 5 kHz when the island is relatively small (poloidal field fluctuations at the edge  $\delta B_{pol} / B_{pol} < 1\%$ ) and decreases to zero if the island grows further. MHD spectrograms show several harmonics of low-frequency oscillations extending up to 20 kHz at most (FIG. 1). Mode analysis at the fundamental frequency gives poloidal number  $m=-2$  and toroidal number  $n=-1$ , where negative mode numbers indicate propagation in the electron diamagnetic

drift direction. Higher harmonics may be due either to the presence of higher spatial harmonics in the island structure, or to non-uniform rotation (“temporal” harmonics). In the discharge shown in FIG. 1 the island appears at  $t=0.1$  s, during current rise; its amplitude progressively grows and harmonics of the “temporal” type appear. During the interval  $0.35 < t < 0.45$  s the island disappears from the spectrogram because its frequency is below the bandwidth of magnetic coils; ECE and soft x-ray diagnostics show that during this interval the island frequency decreases from 100 to 60 Hz at constant amplitude. At  $t=0.45$  s there is an internal disruption, the island amplitude drops and a new cycle of island growth starts.

HF oscillations appear at  $t=0.18$  s; several lines can be distinguished between 30 and 65 kHz (FIG. 1). The two most intense lines have maximum amplitude  $\delta B_{pol}^{HF} / B_{pol} \approx 5 \times 10^{-4}$ ; their frequency difference is exactly twice the fundamental frequency of island oscillations (FIG. 2). As the island amplitude grows, its frequency decreases and the two lines merge; this happens at  $t=0.35$  s and  $t=0.52$  s in FIG. 1.

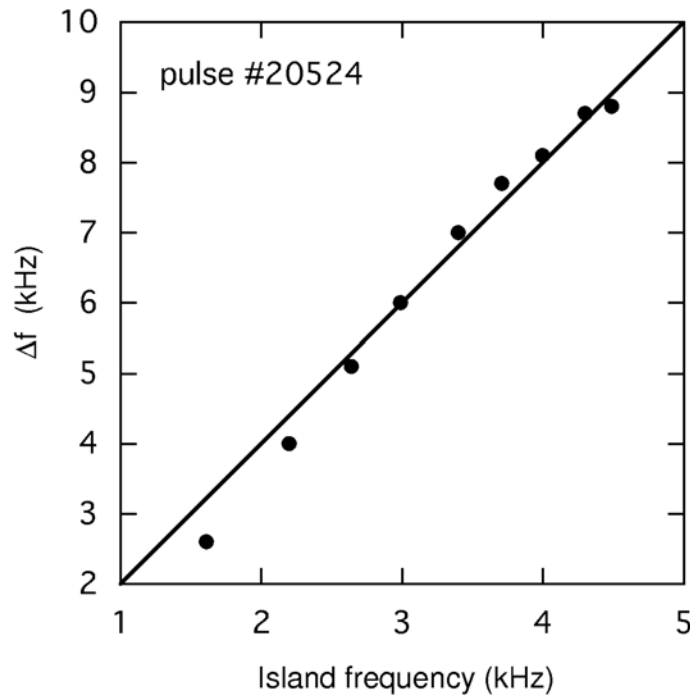


FIG. 2. Frequency difference between the two main HF lines versus the island frequency.

## 2.2. Spatial structure of high-frequency modes

Mode analysis of the two dominant HF lines gives  $n=1$  (i.e. counter-rotation with respect to the island) for the lower frequency line and  $n=-1$  (i.e. co-rotation) for the higher frequency line. These observations imply that, if rotation is purely toroidal, the two HF modes propagate at exactly opposite velocities (and then form a standing wave) in the island rest frame. A slowly drifting standing wave structure can indeed be observed in the amplitude of magnetic signals when the island is large and rotates at very low frequency (FIG. 3). Minima of the envelope correspond with island O and X-points.

The poloidal structure of HF modes is not quite clear; phase analysis of magnetic signals from low field side coils gives  $m=2$  for the  $n=1$  mode and  $m=-2$  for the  $n=-1$  mode, while  $|m|>5$  turns out from high field side coils. The kind analysis used to extract the poloidal structure could be inadequate, since it assumes tearing mode structure, while HF modes could have a different structure, as discussed in Section 3.

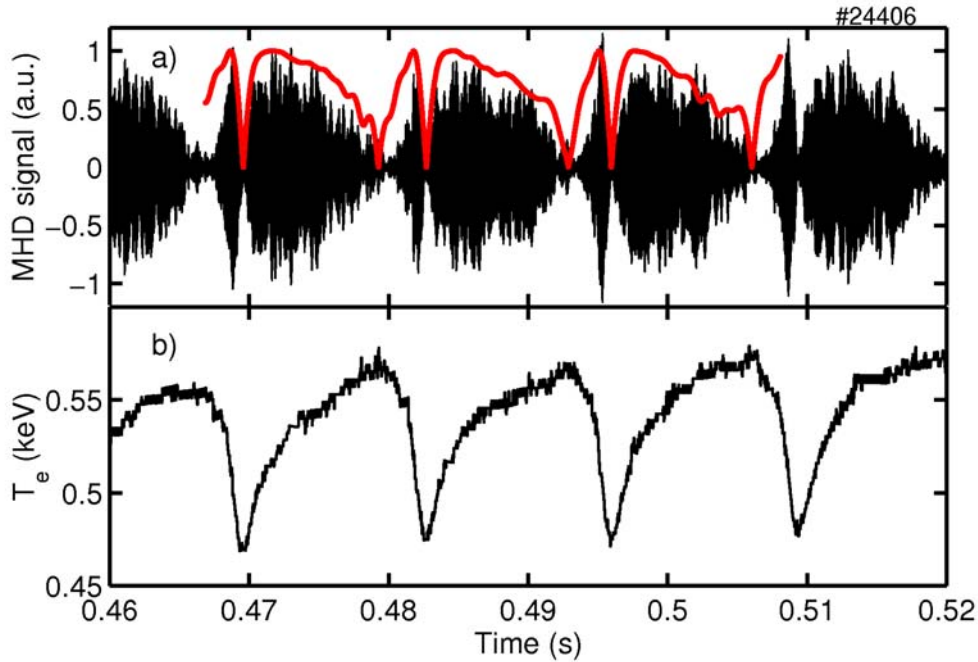


FIG 3. a) HF signals (42-53 kHz) from magnetic coil 5 ( $16^\circ$  above midplane) showing beating structure. b) Temperature oscillations at  $R=0.8$  m from ECE, showing non-uniform island rotation. The red trace in a) shows the beat envelope as evaluated from the phase of signal b).

### 2.3. Influence of island amplitude

HF modes appear if the low-frequency oscillation amplitude exceeds a threshold value of 0.2%. Their frequency increases with island amplitude, as shown in FIG. 4.

HF modes frequency increases by 30% while island amplitude increases by an order of magnitude; at the same time, the island frequency decreases due to electromagnetic torque originated by image currents and field errors. HF mode frequency then increases while island frequency decreases; this excludes any possibility of explaining HF modes as island deformations due for example to toroidal ripple, in fact in this case HF mode frequency would be proportional to island frequency.

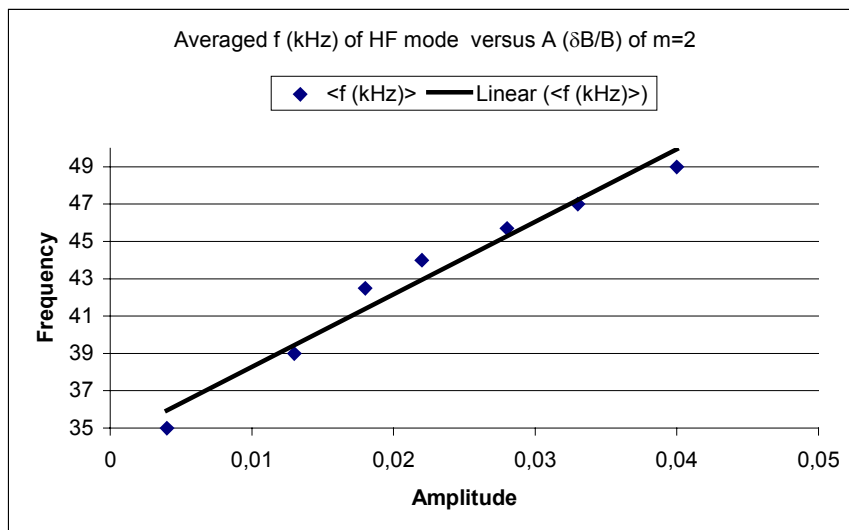


FIG. 4. Frequency of the  $n=-1$  HF mode as a function of tearing mode oscillation amplitude.

### 3. Interpretation

In this section an interpretation of the observed HF modes in terms of Alfvén eigenmodes will be outlined. There are three main experimental features to explain. 1) HF modes only appear when a magnetic island is present. 2) HF modes form standing-wave structures in the island rest frame. 3) HF mode frequencies range from 30 to 70 kHz.

#### 3.1 Island model

A finite-amplitude tearing mode with  $m/n=q_0$  changes the magnetic field topology by forming islands around the radius  $r=r_0$ , where  $q(r_0)=q_0$ . Reconnected field lines form a new set of nested flux surfaces inside the island. These flux surfaces can host new modes that will be periodic in the island angle. Assuming negligible toroidal effects, a single-helicity island can be represented by its (non orthogonal) flux coordinates  $(\kappa, \theta_*, \zeta)$ , where  $\kappa$  is a flux label ( $\kappa=0$  at the O-point and  $\kappa=1$  at the separatrix),  $\theta_*$  is the island angle that spans from 0 to  $2\pi$  around the contours in FIG. 5, and  $\zeta$  is the conventional toroidal angle.

If the tearing perturbation is radially uniform across the island width, simple relationships can be found between island coordinates and conventional helical coordinates  $r, \beta, \zeta$ , where  $\beta = \theta - \zeta/q_0$  and  $\theta$  are helical and poloidal angles respectively [7]. Flux contours in a  $\zeta = \text{const.}$  plane are given by

$$(r - r_0)^2 = w^2 \kappa^2 \text{cn}^2(2K(\kappa)\theta_* / \pi, \kappa), \quad (1)$$

$$\cos(m\beta) = 1 - 2\kappa^2 \text{sn}^2(2K(\kappa)\theta_* / \pi, \kappa), \quad (2)$$

where sn and cn are Jacobi's elliptic functions and K is the complete elliptic integral of the first kind.  $\kappa$ -dependent expressions given in the following hold for  $\kappa < 1$ ; expressions for  $\kappa > 1$  can be found in [7].

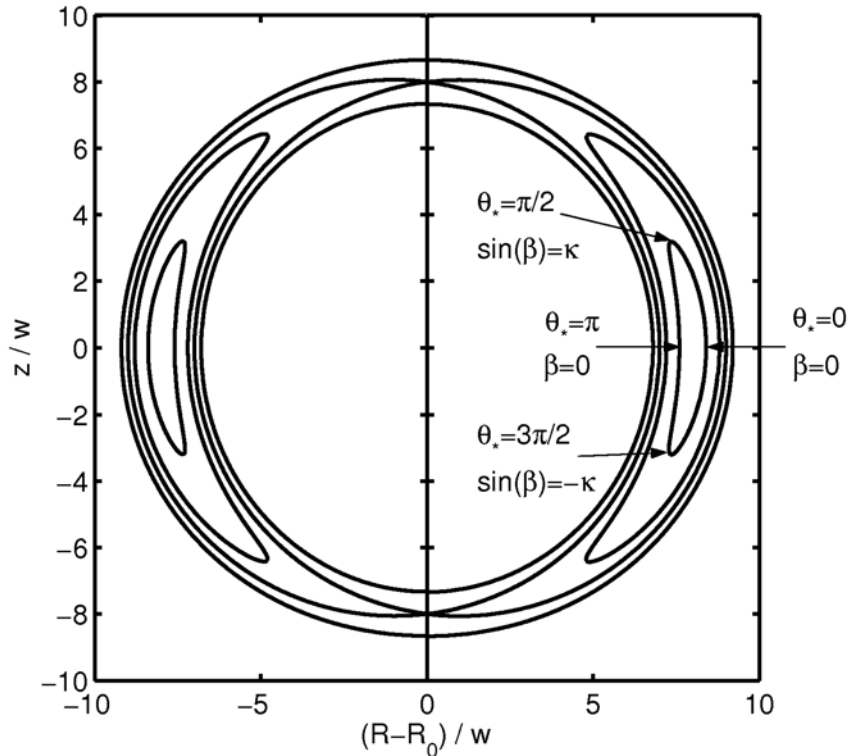


FIG. 5. Schematic of  $m=2$  island flux surfaces with normalised island width  $w/r_0 = 0.125$ . Contours are shown for  $\kappa = 0.4, 0.8, 1.0$  (separatrix) and  $1.2$ .

## 2.2. Mode structure inside the island

Modes inside the island have to be periodic in  $\theta_*$ , so that they will be composed by harmonics of the form  $a_l \exp(il\theta_*)$ . FIG. 6 shows how a pure  $l=2$  harmonic, located on a magnetic surface just inside the island separatrix ( $\kappa=0.999$ ), appears as a function of the helical angle. There is a dominant  $m=2$  structure in  $\beta$ , with strong deformations and discontinuities near  $\pi/2$  and  $3\pi/2$ , where the tips of the selected magnetic surface are located, i.e. near the island X-point. At the magnetic coils location this  $m=2$  dominance will be enforced by propagation effects; however, the difficulty of determining precise mode numbers by standard MHD mode analysis probably depends on phase distortion near the X-points. The  $m=2$  structure in  $\beta$  transforms to  $m=2, n=1$  mode numbers in ordinary toroidal coordinates; this means that the dominant (2,1) and (-2,-1) mode numbers identified for the main HF lines are compatible with  $l=+2$  and  $l=-2$  modes forming a standing wave structure in  $\theta_*$ .

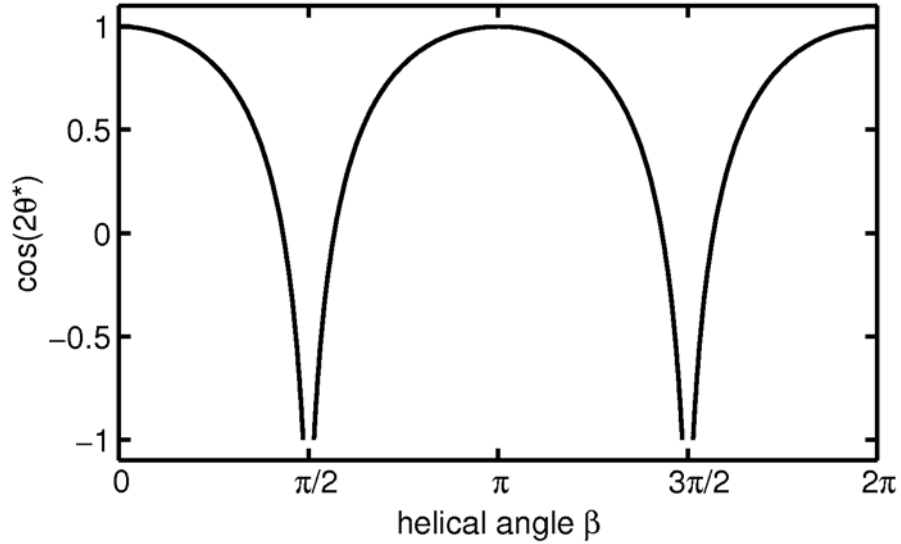


FIG. 6. Island  $\theta_*$  effect near the separatrix ( $\kappa = 0.999$ ). Discontinuities correspond to regions outside island tips.

## 2.3. Alfvén continuum and beta-induced gap in the island

The magnetic field in island coordinates is

$$\mathbf{B} = \nabla \alpha_*(\kappa) \times \nabla (\theta_* - \zeta / q_*) \quad (3)$$

where  $\alpha_*(\kappa)$  is a generalised toroidal flux and the island winding index

$$q_* = (4/\pi)(q_0/ms)(r_0/w)K(\kappa) \quad (4)$$

is inversely proportional to field lines inclination with respect to the helical direction, e.g.  $q_*$  diverges at the separatrix (FIG. 7), where field lines are exactly in the helical direction. Here  $s$  and  $w$  are magnetic shear at  $r_0$  and island half width respectively. For a wave with periodicity  $l$  the parallel wavenumber is  $k_{\parallel} = l/Rq_*$ ; the corresponding Alfvén frequencies

$$f = k_{\parallel} V_A / 2\pi = l V_A / 2\pi R q_* \quad (5)$$

are shown in FIG. 8.

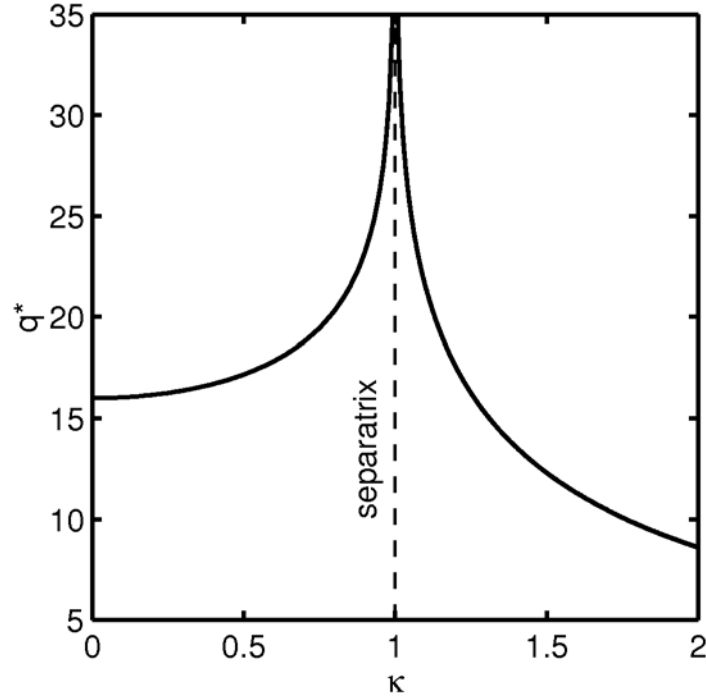


FIG. 7.  $q^*$  dependence on the island flux coordinate  $\kappa$  ( $\kappa=0$  at  $O$ -point;  $\kappa=1$  at separatrix), with  $q_0 = 2$ , mode number  $m = 2$ , magnetic shear  $s = 1$  and normalised island width  $w/r_0 = 0.125$ .

The continuum represented by (5) differs in several respects from the one found in the cylindrical limit of an axisymmetric equilibrium. First, the spatial structure is different, in fact the  $k_{\parallel} = 0$  line at  $r = r_0$  that characterises cylindrical geometry splits along the island separatrix and takes a steeper slope around it (FIG. 7). Second, the metric coefficients are not constant on magnetic surfaces, i.e. they depend on  $\theta_*$ , for example

$$|\nabla \alpha_*|^2 \approx q_*^2 B_0^2 (s/q_0)^2 w^2 \kappa^2 (\text{cn}^2 + (m/4)^2 (w/r_0)^2 \text{sn}^2 \text{dn}^2) \quad (6)$$

where the elliptic functions sn, cn and dn have arguments  $(2K(\kappa)\theta_*/\pi, \kappa)$ . In particular the term proportional to  $(w/r_0)^2$  gives rise to components of the form  $\exp(4i\theta_*)$ , which can couple modes with  $l=+2$  and  $l=-2$ , i.e. modes that can form a standing wave like the experimentally observed one.

The island continuum is broken as it merges into the beta-induced Alfvén gap. Keeping into account ion compressibility effects, the frequency continuum accumulation point is given by [3]

$$\omega_{\beta} = (7/4 + T_e/T_i)^{1/2} q_0 \omega_{ii}, \quad (7)$$

where  $\omega_{ii} = \sqrt{2T_i/m_i}/q_0 R_0$  is the ion transit frequency. Diamagnetic effects have been neglected in (7) since  $\omega_{\beta}$  is much larger than ion pressure and density diamagnetic frequencies [3]. The accumulation point is shown as a dashed line in FIG. 8. The grey area in the same figure represents the range of measured frequencies for the main HF modes. The fact that HF modes are positioned near the top of the beta-induced gap points to their identification as BAE modes. Calculation of mode structure to be compared with experimental observations and determination of the driving mechanism in the presence of the magnetic island are left to a future work.

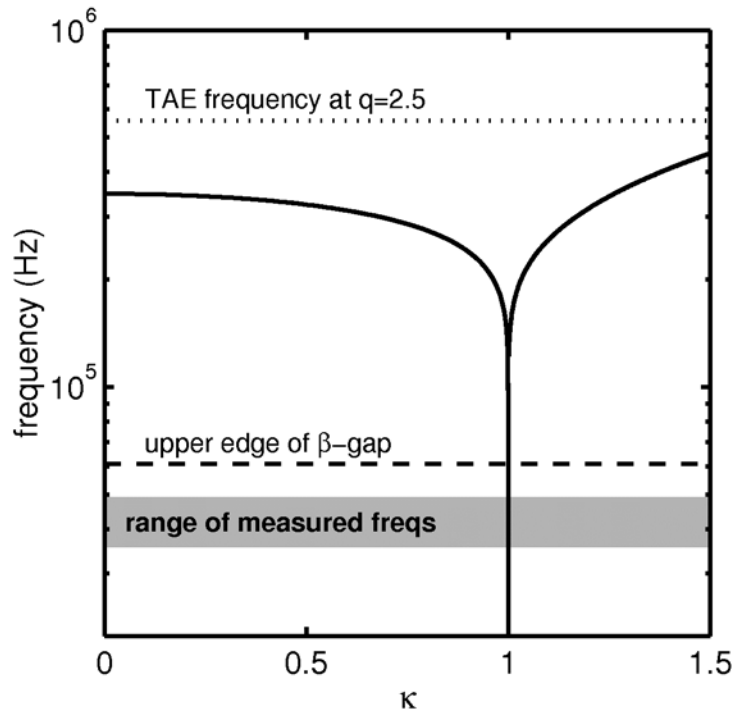


FIG. 8. Continuum and gap frequencies, calculated with  $q_0 = 2$ ,  $m = 2$ ,  $s = 1$ ,  $w/r_0 = 0.125$ ,  $B = 5.9$  T,  $n_i = 3 \times 10^{19} \text{ m}^{-3}$ ,  $T = 0.5$  keV. Tearing modes lie below the baseline (20 kHz).

#### 4. Conclusions

The main conclusion of this work is that the development of magnetic islands can open new channels of instability to Alfvén eigenmodes. High-frequency modes observed in ohmic plasmas at the boundary of the beta-induced Alfvénic gap have been interpreted as beta-induced Alfvén eigenmodes, which develop near the separatrix of magnetic islands. The observed HF modes saturate at very small amplitudes in ohmic plasmas, where energetic ions are absent, but they could become a new loss mechanism in the presence of fusion-generated alpha particles. The existence of such a loss mechanism could be verified in experiments where fast ions can be accelerated by ion cyclotron resonance heating, and where magnetic islands can be generated in a controllable way, either by neoclassical tearing modes or by external helical perturbations.

#### References

- [1] TURNBULL, A.D., et al., "Global Alfvén modes: Theory and experiment", Phys. Fluids **B5** (1993) 2546.
- [2] HEIDBRINK, W.W., et al., "Observation of Beta Induced Alfvén Eigenmodes in the DIII-D Tokamak", Phys. Rev. Lett. **71** (1993) 855.
- [3] ZONCA F., et al., "Kinetic theory of low-frequency Alfvén modes in tokamaks", Plasma Phys. Contr. Fusion **38** (1996) 2011.
- [4] ZONCA F., et al., "Existence of ion temperature gradient driven shear Alfvén instabilities in tokamaks", Phys. Plasmas **6** (1999) 1917.
- [5] SHARAPOV, S.E., et al., "Experimental studies of instabilities and confinement of energetic particles on JET and on MAST", this Conference, paper EX/5-2Ra.
- [6] BURATTI, P., et al., "MHD activity in FTU plasmas with reversed magnetic shear", Plasma Phys. Contr. Fusion **39** (1997) B383.
- [7] SWARTZ, K. and HAZELTINE, R.D., Phys. Fluids **27** (1984) 2043.